RAA 2015 Vol. **15** No. **11**, 1881–1892 doi: 10.1088/1674–4527/15/11/010
http://www.raa-journal.org *http://www.iop.org/journals/raa*

Research in Astronomy and Astrophysics

Payload topography camera of Chang'e-3

Guo-Bin Yu, En-Hai Liu, Ru-Jin Zhao, Jie Zhong, Xiang-Dong Zhou, Wu-Lin Zhou, Jin Wang, Yuan-Pei Chen and Yong-Jie Hao

Institute of Optics and Electronics, Chinese Academy of Sciences, Chengdu 610209, China; *ygb@ioe.ac.cn*

Received 2014 July 21; accepted 2015 May 19

Abstract Chang'e-3 was China's first soft-landing lunar probe that achieved a successful roving exploration on the Moon. A topography camera functioning as the lander's "eye" was one of the main scientific payloads installed on the lander. It was composed of a camera probe, an electronic component that performed image compression, and a cable assembly. Its exploration mission was to obtain optical images of the lunar topography in the landing zone for investigation and research. It also observed rover movement on the lunar surface and finished taking pictures of the lander and rover. After starting up successfully, the topography camera obtained static images and video of rover movement from different directions, 360° panoramic pictures of the lunar surface around the lander from multiple angles, and numerous pictures of the Earth. All images of the rover, lunar surface, and the Earth were clear, and those of the Chinese national flag were recorded in true color. This paper describes the exploration mission, system design, working principle, quality assessment of image compression, and color correction of the topography camera. Finally, test results from the lunar surface are provided to serve as a reference for scientific data processing and application.

Key words: Moon — instrumentation: detectors — techniques: image processing

1 INTRODUCTION

Chang'e-3 was China's first lunar probe that achieved a soft landing and performed a roving exploration on the lunar surface. It was composed of a lunar probe that soft landed on the surface (hereinafter referred to as the "lander") and a lunar roving probe (hereinafter referred to as the "rover"). The scientific goals of Chang'e-3 included (1) lunar surface topography and geology survey, (2) lunar surface material composition and resource survey, and (3) Earth plasma layer detection and lunar-based ultraviolet astronomy observation (Ye & Peng 2006). The Chang'e-3 probe was successfully launched by a "Long March-III B Model 2" rocket at 17:30 on 2013 December 1 (UTC) and smoothly landed at the landing point (19.51°W, 44.12°N) in Sinus Iridum at 13:11 (UTC) on 2013 December 14 (Li et al. 2014; Ip et al. 2014; Liu et al. 2014), which initiated the exploration mission associated with China's first lunar soft landing. After the Chang'e-3 probe successfully landed on the lunar surface, the four payloads installed on the lander were activated for in-situ investigation, and the four payloads installed on the rover were used for roving exploration in order to complete the scientific exploration mission (Dai et al. 2014).

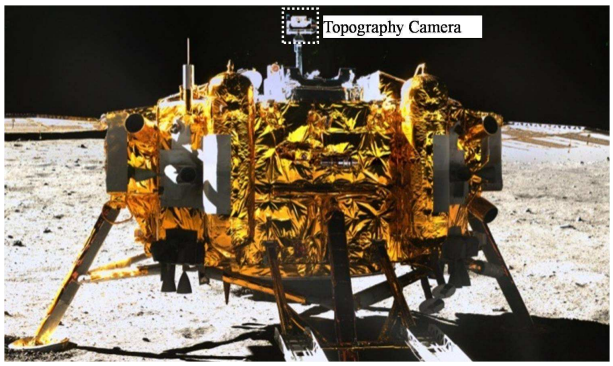

Fig. 1 Photograph of the lander with the topography camera identified.

The topography camera was one of the main scientific payloads installed on the lander. In order to best utilize the designed capability of the camera pointing mechanism and to ensure a normal range of operating temperature, the camera adopted a split design. It was composed of a camera, an electronic component that performs image compression, and a cable assembly. The camera was installed on a two-dimensional turntable such that the camera pointing mechanism was mounted at the top of the lander and could easily acquire images, as shown in Figure 1. The electronic component that performed image compression was integrated into the lander's payload electrical control box. The cable assembly was routed to the camera and the electronic component that performed image compression through the inner wall of the camera pointing mechanism. To improve the demonstration capability of scientific exploration results and engineering implementation, the Chang'e-3 topography camera was designed with color imaging capability, which could obtain color images of the rover. The topography camera obtained optical image data of the lunar surface in the landing zone and color image data of the rover at an azimuth of $\pm 175^\circ$ (the imaging coordinate system is the same coordinate system that was used the lander, where an azimuth of 0° coincides with the $+Z$ axis of the lander) and a pitch angle of $\pm$ 60° (a pitch angle of 0° is the plane defined by the Y-Z axis of the lander) relative to the lunar surface.

In Section 2, the scientific exploration goals of the Chang'e-3 topography camera are first introduced. Then in Section 3, the functions and performance are given. In Section 4, the working principle and system design are described. In Section 5, the assessment of image compression quality and color correction are provided. Lunar surface exploration mission objectives are provided in Section 6 and conclusions are given in Section 7.

2 SCIENTIFIC EXPLORATION GOALS

The topography camera operated together with other payloads to accomplish the lunar surface topography and geology survey. The goal of the scientific exploration mission using the topography camera was to obtain optical images of the lunar surface topography in the landing zone for investigation and research. The engineering exploration task was to acquire color pictures of the rover (including pictures of China's national flag), complete mutual picture-taking, monitor and record rover movement, and improve engineering demonstration capability.

3 FUNCTIONS AND PERFORMANCE

The topography camera was able to: (1) obtain images of the lunar surface in the landing zone and monitor rover movement on the lunar surface; (2) acquire color images; (3) take static images and video; (4) adjust exposure; (5) protect against dust; (6) compress images; (7) reduce stray light.

Table 1 Main Characteristics of the Topography Camera

No.	Parameter	Value
1	Wavelength range	Visible light
2	Color	Color (R, G, B)
3	Imaging mode	Static and video (switchable)
4	Normal imaging distance (m)	5 to ∞
5	Effective pixels	2352×1728
6	Field of view (FOV) angle	$22.9^\circ \times 16.9^\circ$
7	Frame frequency (fps)	5
8	Quantized value (bit)	8
9	Signal-to-noise ratio (dB)	49.5 (max.)
		36 (albedo: 0.09, solar elevation angle: 30°)
10	System static MTF	0.25 (full FOV)
11	Image compression peak signal-to-noise ratio (dB)	Static image PSNR $\geq$ 46
12	Image compression	2:1 (static imaging)
		24:1 (video imaging)
13	Power consumption (W)	3.5 (camera)
14	Weight (kg)	0.58 (camera)

The topography camera was kept inactive when the Chang'e-3 probe was being launched, in the Earth-Moon transfer orbit, lunar orbit, and landing. It was activated after the lander landed safely and the rover was separated from the lander. Table 1 lists the main characteristics of the topography camera. It could operate in either standby mode or detection mode (static camera, sampling video camera, and window video camera).

Standby mode: The camera was in a power-on state without actively acquiring a picture. No image data were output during the initial power-on state.

Detection mode: The camera was in a power-on state while actively acquiring a picture. The camera provided three switchable detection modes, including the static mode (Frame frequency: 1 frame/2.5 s, Resolution: 2352×1728), sampling video mode (Frame frequency: 5 frame/second, Resolution: 720×576, 720×576 obtained by downsampling of 2352×1728 resolution), and window video mode (Frame frequency: 5 frame/second, Resolution: 720×576, 720×576 obtained by window acquisition of 2352×1728 resolution). After completion of the static mode, the camera automatically returned to the standby mode. The two video modes could be switched to static mode, and could be switched to each other.

4 WORKING PRINCIPLE AND SYSTEM DESIGN

4.1 System Composition

The topography camera adopted a split design, as shown in Figure 2. Its camera was mounted on the two-dimensional turntable of the camera pointing mechanism at the top of the lander. The electronic component that performed image compression was integrated in the electrical control box for the payload of the lander. The cable assembly was routed to the camera and electronic component that performed image compression through the inner wall of the camera pointing mechanism. Hardware that was part of the topography camera was made up of the camera, an electronic component used for image compression, and cable assembly. Additional hardware was comprised of a Field-Programmable Gate Array (FPGA) used for camera control and an FPGA for image compression.

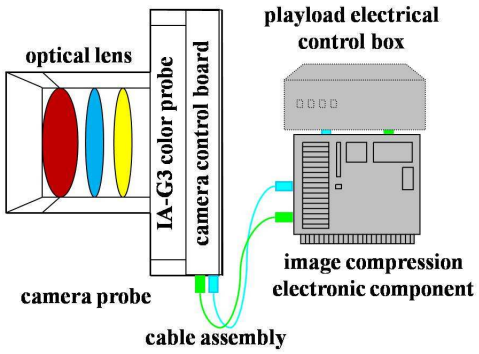

Fig. 2 Schematic diagram of system design and working principle.

4.2 Working Principle

An optical lens of the topography camera collected optical signals that contained imaging targets (lunar topography, rover) and created an image on the IA-G3 color sensor, which then converted optical signals into image data, as shown in Figure 2. The camera control board sent the original image data to the electronic component used for image compression at a rate of 24 Mbps. The electronic component used for image compression compressed the original image data and then redirected the compressed code stream to the data management subsystem.

The camera control FPGA located on the camera control board was responsible for driving the IA-G3 color sensor, collecting original image data, communicating via an RS-422 interface, and transmitting original image data to the image compression FPGA.

The image compression FPGA located on the electronic component that performed image compression communicated via RS-422 and sent the compressed code stream to the data management subsystem.

When the topography camera was used to take static images, its frame frequency was set to 1 frame/2.5 s, resolution to 2352×1728, image compression ratio to 2:1, and transmission rate to 8 Mbps.

When the topography camera was used to acquire video, its frame frequency was set to 5 frame/second, resolution to 720×576, image compression ratio to 24:1, and transmission rate to 800 kbps. The topography camera generated images with a resolution of 720×576 using one of the two modes: window acquisition and downsampling.

Commands and data to the topography camera were sent by using the lander's electrical control box for the payload to transmit data packets to the image compression FPGA through an RS-422 serial interface. After receiving data packets, the image compression FPGA forwarded data packets related to the camera to the camera control FPGA inside the camera. Engineering parameters of the topography camera were sent by using the image compression FPGA to the lander's payload electrical control box through the RS-422 interface.

4.3 System Design

4.3.1 Probe selection

Based on the function and performance requirements, and the requirements for lighting, temperature, and irradiation based on the environment of the lunar surface, the topography camera used DALSA company's IA-G3 color sensor. Its main characteristics were as follows: (1) spectral response range:

400 nm to 1100 nm, (2) effective pixel number: 2352×1728, (3) pixel size: $7.4 \times 7.4\ \mu m^2$, (4) frame frequency: 62 frame/second, (5) full trap charge: 60 000 e, (6) anti-vignetting factor: 1000, and (7) operating temperature: –40°C to +60°C.

4.3.2 Optical system and lens design

As the topography camera was the "eye" of the lander, it must be able to operate in the particular conditions on the lunar surface, such as cosmic rays, extreme cold or hot temperatures, and lighting conditions. If the camera's ability to operate in these conditions was inadequate, the cosmic rays on the lunar surface would be detrimental to the transmittance capability of the optical lens, which would significantly hamper the functionality of the topography camera. The optical system utilized technology that helped it function even when radiation was in this environment and all anti-radiation optical materials ensured that the topography camera could properly acquire images (Nicoletta & Eubanks 1972). Moreover, due to dramatic changes in temperature on the lunar surface, the optical lenses must be able to withstand extreme temperatures that range from –180°C to +150°C, and operate properly in a thermal vacuum environment with temperatures ranging from –35°C to +65°C. With advanced designs, such as passive thermalization in the optical systems, the optical lenses could adapt to the particular temperature conditions on the Moon, ensuring high image quality and guaranteeing that the topography camera could see clearly. In addition, how to take "true color" photographs on the Moon had been a challenge for designers and engineers. After extensive consideration, calculation, and experiments, the cutoff wavelength range of the optical lenses was ultimately determined to ensure that the topography camera could acquire as realistic images as possible.

The main technical parameters of the optical system that was part of the topography camera were: (1) wavelength range: 420 nm to 700 nm, (2) field of view: $22.9^\circ \times 16.9^\circ$, (3) clear aperture: 5.4 mm, (4) focal length: 43 mm, (5) f-number: 8, (6) imaging distance: 5 m to ∞, (7) modulation transfer function (MTF): > 0.45, (8) spectral transmittance: $> 85\%$, and (9) operating temperature: –35°C to +65°C. The wave band of the optical system was designed to be from 420 nm to 700 nm, the central wavelength 540 nm, the diagonal field of view 28.2°, the optical volume $\Phi 23 \times 38.5\ mm^2$, and the optical weight 15 g. The structural design of the optical lenses is shown in Figure 3.

4.3.3 Structural design of the camera

When designing the structure of the topography camera, the following were mainly considered: (1) mechanical environment conditions of launch, transfer, and landing, (2) imaging quality requirements of the optical system, (3) lightweight and compact structure design requirements, and (4) thermal control requirements of the probe. The camera consisted of an optical lens assembly, box, rear box, active pixel sensor (APS) circuit board, camera control board, and cover. Based on the relationship between the APS circuit board and the optical lenses, the APS circuit board was fixed perpendicularly to the optical lenses while being parallel to the camera control board so that between the two boards there would be sufficient space for components and connectors. The clear aperture in the light shield of the optical lenses was a tapered square hole (as shown in Fig. 4), which not only reduced stray light outside the field of view, yielding improved image quality, but also protected the optical lenses from lunar dust. To reduce heat generated by the surface-mounted APS probe during operation, the camera used a special I-shaped thermal conductive device and heat conduction path to transfer generated heat to the camera's mechanical structure, which would then transfer the heat to the optical solar reflector (OSR) thermal film on the heat dissipation panel in order to dissipate heat into deep space. The heat dissipation area of the OSR film was $105 \times 80\ mm^2$. This design solved the heat dissipation problem of the high-power surface-mount APS probe, ensuring a good temperature difference between the APS probe and the camera's mechanical structure. The ability to sustain this

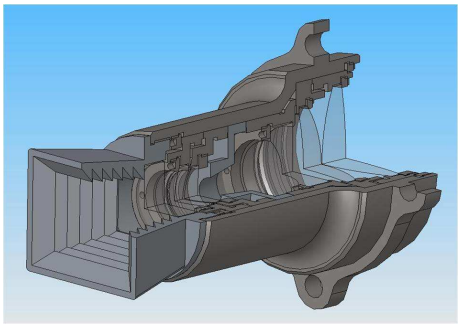

Fig. 3 Structural design of optical lenses.

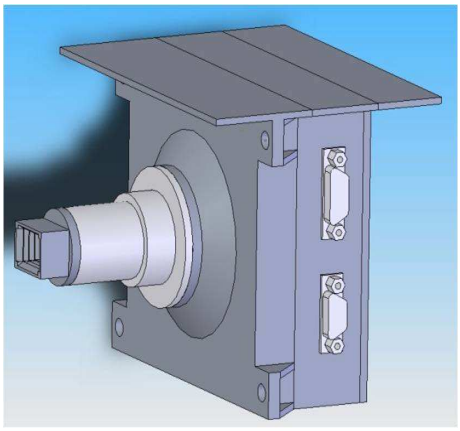

Fig. 4 Schematic diagram of the camera.

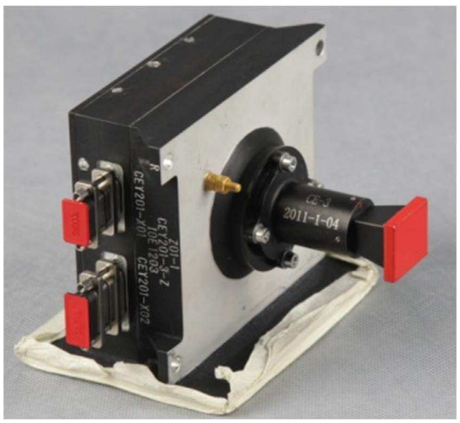

Fig. 5 Photograph of the camera.

temperature difference at 5°C allowed the camera to work at a high temperature of 150°C. Figure 4 shows a schematic diagram of the camera, and Figure 5 shows a photograph of the camera.

5 ASSESSMENT OF IMAGE COMPRESSION QUALITY AND COLOR CORRECTION

5.1 Assessment of Image Compression Quality

The topography camera implemented image compression algorithms using an FPGA. In order to verify the performance and effectiveness of the FPGA, the actual color images of the lunar surface and those of positive samples were used to evaluate the image compression quality (Zhao R. J. et al. 2015 in preparation). The "difference" between the corresponding pixels of the original image and the decompressed image were obtained using a quantitative calculation, which allowed for measuring the similarity between the original image and the decompressed image. The most commonly used evaluation standards are mean square error (MSE) and peak signal to noise ratio (PSNR). The MSE calculation formula is shown in Equation (1), and it incorporates the average gray deviation between the original image and decompressed image. Under normal circumstances, a smaller MSE value leads to a better decompressed image.

$$\mathrm{MSE} = \frac{1}{XY}\sum_{x=1}^{X}\sum_{y=1}^{Y}\left[f(x,y) - f'(x,y)\right]^2. \quad (1)$$

PSNR was used to evaluate the quality of the decompressed image by calculating the ratio between the signal peak value and the MSE value. The measurement unit is decibel (dB) and its formula is shown in Equation (2).

$$\mathrm{PSNR} = 20 \lg \frac{255}{\sqrt{\frac{1}{XY} \sum_{x=1}^{X} \sum_{y=1}^{Y} \left[f(x,y) - f'(x,y) \right]^2}}. \tag{2}$$

In Equations (1) and (2), $f(x,y)$ indicates the gray value of the original image, $f'(x,y)$ represents the gray value of the decompressed image, (x,y) denotes image pixel coordinates, X indicates the maximum values of image pixel coordinates of the horizontal coordinate and Y signifies the maximum values of image pixel coordinates of the longitudinal coordinate.

The PSNR is calculated between the original image and the decompressed image using the same color interpolation. The PSNR value of the decompressed image satisfies the requirement for the topography camera (PSNR$\geq$45), as shown in Figures 6 to 8.

5.2 Assessment of Color Correction

Inconsistency between the color spectral response function of the IA-G3 color sensor used by the topography camera and the color matching function of the International Commission Illumination (CIE) 1931 standard observer (GB/T 3977-2008[1]; Valous et al. 2009), and impact of the lunar surface lighting conditions on camera color responsiveness would cause color cast in images taken by the topography camera. To deal with those problems, a two-step color correction method that combined color calibration and white balance was designed (Zhao R. J. et al. 2015 in preparation). First, to calibrate the inconsistency between the camera color spectral response function of the IA-G3 color sensor and the color matching function of the CIE-1931 standard observer, the camera's RGB chromaticity response correction matrix under the RGB color system was obtained by using the least squares adjustment of the 24-color cards under D65, which also improved the applicability of the correction matrix to different color images. Secondly, under various lighting conditions close to those in the environment of the lunar surface, the least squares adjustment of the n-order neutral color cards was adopted for the camera's white balance correction, which improved the generalization ability of the traditional single-color white balance correction coefficient and effectively reduced the impact of lunar surface lighting conditions on the camera's image color (Ren et al. 2014).

Color correction accuracy is mainly evaluated through the two measures of color calibration error and white balance correction error.

$$\Delta E_{\mathrm{ori}}^{\mathrm{rgb}} = \frac{\sum\limits_{k=1\cdots24} [(r_{\mathrm{std}} - r_{\mathrm{ori}})^2 + (g_{\mathrm{std}} - g_{\mathrm{ori}})^2 + (b_{\mathrm{std}} - b_{\mathrm{ori}})^2]^{1/2}}{24}, \tag{3}$$

$$\Delta E_{\mathrm{cor}}^{\mathrm{rgb}} = \frac{\sum\limits_{k=1\cdots24} [(r_{\mathrm{std}} - r_{\mathrm{cor}})^2 + (g_{\mathrm{std}} - g_{\mathrm{cor}})^2 + (b_{\mathrm{std}} - b_{\mathrm{cor}})^2]^{1/2}}{24}. \tag{4}$$

In Equations 3 and 4, $\Delta E_{\mathrm{ori}}^{\mathrm{rgb}}$ indicates the average chromaticity value of 24-color cards before color calibration, $\Delta E_{\mathrm{cor}}^{\mathrm{rgb}}$ represents the average chromaticity value of 24-color cards after color calibration, r_{std}, g_{std}, b_{std} denote standard chromaticity values of color codes, r_{ori}, g_{ori}, b_{ori} signify chromaticity values of color codes before color calibration, and r_{cor}, g_{cor}, b_{cor} give chromaticity values of color code after color calibration.

$$\Delta E_{\mathrm{ori}}^{\mathrm{white}} = \frac{\sum\limits_{k=1\cdots n} [(r'_{\mathrm{ori}} - 1/3)^2 + (g'_{\mathrm{ori}} - 1/3)^2 + (b'_{\mathrm{ori}} - 1/3)^2]^{1/2}}{n}, \tag{5}$$

[1] GB/T 3977–2008, Methods for the measurement of object color (Standardization Administration of The People's Republic of China).

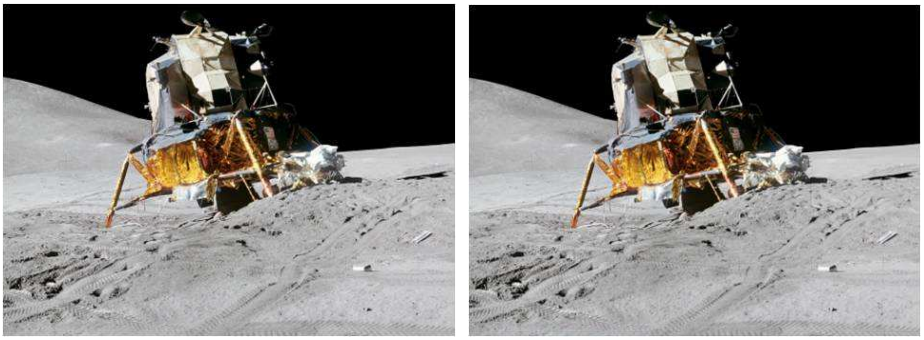

Fig. 6 *Left*: Before; *right*: After. Contrast between lunar surface color images before and after compression (MSE = 0.63, PSNR = 50.11).

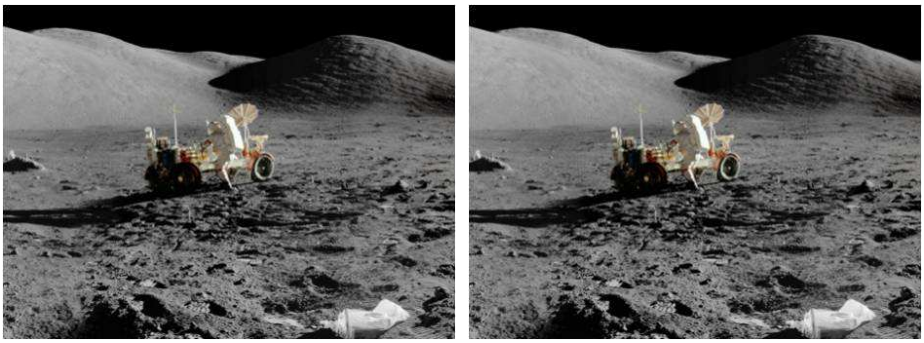

Fig. 7 *Left*: Before; *right*: After. Contrast between lunar surface color images before and after compression (MSE = 1.35, PSNR = 46.83).

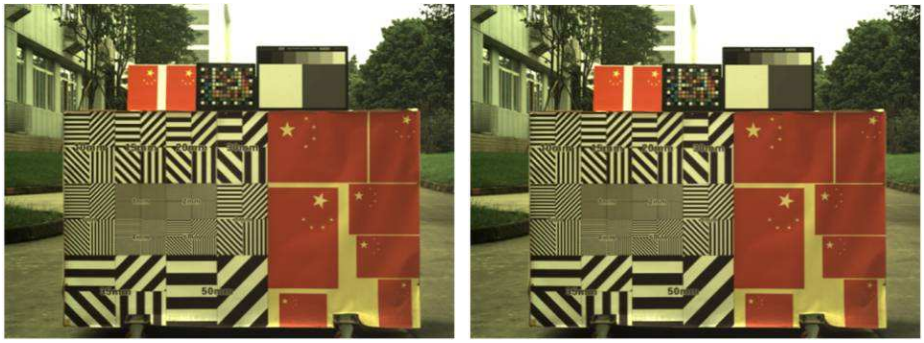

Fig. 8 *Left*: Before; *right*: After. Contrast between positive sample images before and after compression (MSE = 0.99, PSNR = 48.18).

$$\Delta E_{\mathrm{cor}}^{\mathrm{white}} = \frac{\sum\limits_{k=1\cdots n} [(r'_{\mathrm{cor}} - 1/3)^2 + (g'_{\mathrm{cor}} - 1/3)^2 + (b'_{\mathrm{cor}} - 1/3)^2]^{1/2}}{n}. \tag{6}$$

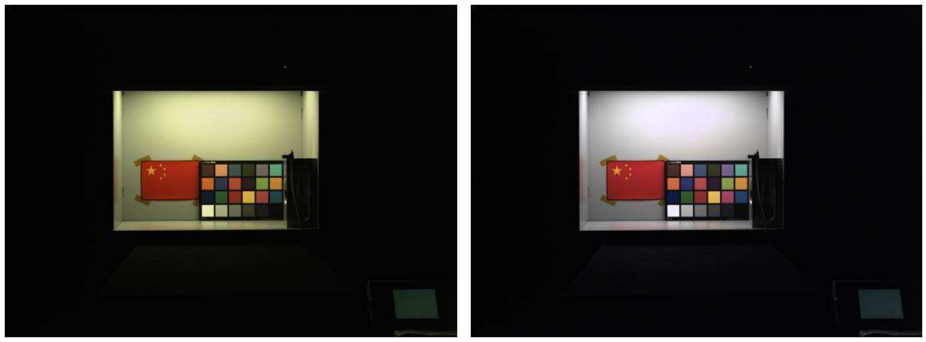

Fig. 9 *Left*: ($\Delta E_{\mathrm{ori}}^{\mathrm{rgb}} = 0.0647$), *Right*: ($\Delta E_{\mathrm{cor}}^{\mathrm{rgb}} = 0.046$). Contrast between images of the Chinese flag taken under the indoor D65 light source before and after color calibration.

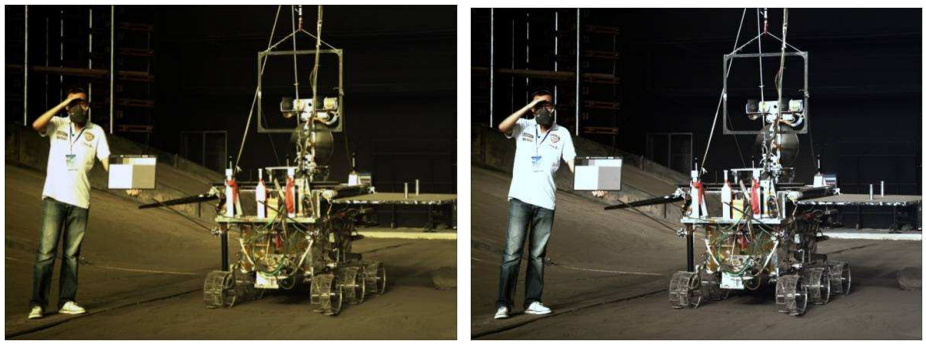

Fig. 10 *Left*: ($\Delta E_{\mathrm{ori}}^{\mathrm{white}} = 0.0749$), *Right*: ($\Delta E_{\mathrm{cor}}^{\mathrm{white}} = 0.00188$). Contrast between images of the rover taken under simulated lunar surface lighting conditions before and after white balance correction.

In Equations 5 and 6, $\Delta E_{\mathrm{ori}}^{\mathrm{white}}$ indicates the average chromaticity value of n-order neutral color cards before white balance correction, $\Delta E_{\mathrm{cor}}^{\mathrm{white}}$ signifies the average chromaticity value of n-order neutral color cards after white balance correction, r'_{ori}, g'_{ori}, b'_{ori} represent chromaticity values of color code before white balance correction, and r'_{cor}, g'_{cor}, b'_{cor} give chromaticity values of color code after white balance correction.

The ground tests of color correction are shown in Figures 9 and 10. Under the D65 light source and simulated lunar surface lighting conditions, both color cards and colors were significantly restored, leading to a higher approximation to the actual colors that human eyes could see. Especially in the simulated lunar surface lighting environment, the rover color was effectively improved, indicating that the white balance correction had eliminated the impact of lunar surface illumination and thus was more applicable to lunar surface imaging.

6 LUNAR SURFACE EXPLORATION MISSION OBJECTIVES

At 21:11 on 2013 December 14, the Chang'e-3 lunar probe successfully soft landed on the lunar surface. After the lander and rover separated, the topography camera was used to explore the lunar surface. The main exploration mission objectives completed on the lunar surface included: (1) taking static images and video of rover movement from different angles and capturing pictures of the lander

Fig. 11 First picture of the lunar surface after powering up (taken at 05:58:12 on 2013 December 15).

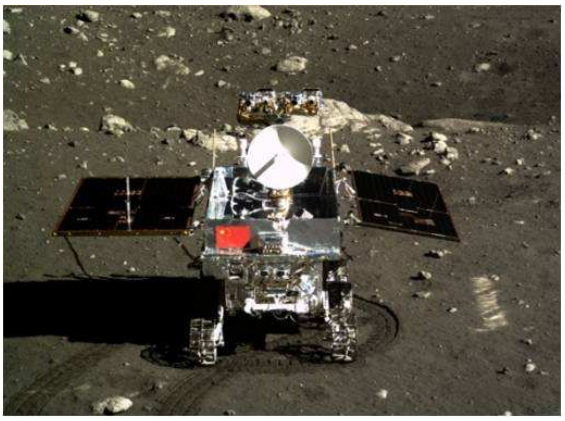

Fig. 12 Picture of the rover at point A (taken at 23:42:16 on 2013 December 15).

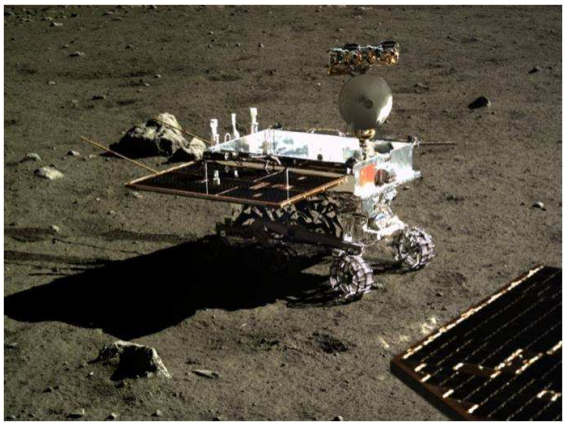

Fig. 13 Picture of the rover at point B (taken at 04:59:04 on 2013 December 16).

Fig. 14 Picture of the lunar surface in the landing zone (taken at 00:24:59 on 2013 December 18).

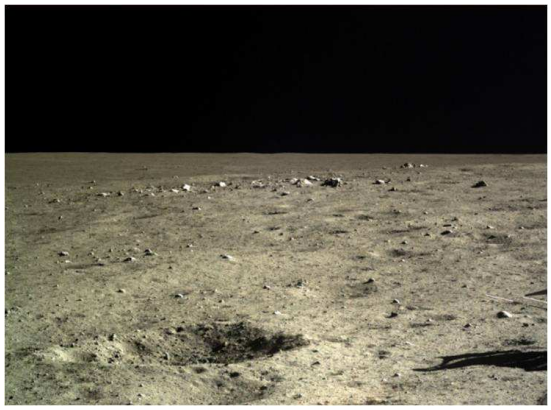

Fig. 15 Picture of the lunar surface in the landing zone (taken at 10:22:43 on 2013 December 23).

Fig. 16 Picture of the Earth (taken at 02:19:50 on 2013 December 25).

and rover, (2) taking 360° panoramic images of the lunar surface topography in the landing zone from multiple angles, and (3) shooting a number of pictures of the Earth. The topography camera successfully fulfilled all assigned scientific and engineering exploration mission objectives.

Representative images of the lunar surface acquired by the topography camera are shown in Figures 11 to 16. The topography camera took clear images of the rover, lunar surface and the Earth, and showed the true color of the national flag of China. Photos of the Earth allowed us to see the planet from another point of view.

7 CONCLUSIONS

The topography camera was the main payload on the Chang'e-3 lander. It accomplished mission objectives including obtaining optical images of the landing zone topography and observing the rover and its movement on the lunar surface, providing image data for research on lunar surface topography and geological structure, and taking pictures of both the lander and the rover. Before launch, ground tests, assessment of image compression quality, assessment of color correction, and environmental simulation tests were conducted for the topography camera. After successfully powering up on the lunar surface at 05:58:12 on 2013 December 15, the topography camera took static pictures and video of rover movement from different angles, 360° panoramic shots of the lunar surface topography in the landing zone from multiple angles, and numerous pictures of the Earth. All photos and videos of the rover, lunar surface, and the Earth were clear, and those of the Chinese national flag showed the true color.

Acknowledgements We give special thanks to the special funds of Phase 2 of the Chinese Lunar Exploration program for supporting this work. We also give special thanks for the strong support from the leadership and colleagues in the Moon and Deep Space Exploration Ground Application System Department of the Chinese Academy of Sciences for help in developing the camera. We also thank the strong support and assistance from the Moon and Deep Space Exploration Ground Application System Department of the Chinese Academy of Sciences for ground test validation and data preprocessing. In addition, we give special thanks for the strong support and help from the Overall Payload Space Center of the Chinese Academy of Sciences in camera development and joint tests, and special thanks to researchers from Institute 8358 of China Aerospace Science and Industry Corporation and those from Xi'an University of Electronic Science and Technology.

References

Dai, S., Jia, Y., Zhang, B., et al. 2014, Sci. Sin. Tech, 44, 361
Ip, W.-H., Yan, J., Li, C.-L., & Ouyang, Z.-Y. 2014, RAA (Research in Astronomy and Astrophysics), 14, 1511
Li, C.-L., Mu, L.-L., Zou, X.-D., et al. 2014, RAA (Research in Astronomy and Astrophysics), 14, 1514
Liu, J.-J., Yan, W., Li, C.-L., et al. 2014, RAA (Research in Astronomy and Astrophysics), 14, 1530
Nicoletta, C. A., & Eubanks, A. G. 1972, Appl. Opt., 11, 1365
Ren, X., Li, C.-L., Liu, J.-J., et al. 2014, RAA (Research in Astronomy and Astrophysics), 14, 1557
Valous, N. A., Mendoza, F., Sun, D.-W., & Allen, P. 2009, Meat Science, 81, 132
Ye, P. -J., & Peng, J. 2006, China Engineering Science, 8, 13